Article

Observation of Dynamic Solvent Effect for Electron Tunneling in U-Shaped Molecules

Min Liu, David H. Waldeck, Anna M. Oliver, Nicholas J. Head, and Michael N. Paddon-Row

J. Am. Chem. Soc., **2004**, 126 (34), 10778-10786• DOI: 10.1021/ja049539d • Publication Date (Web): 06 August 2004

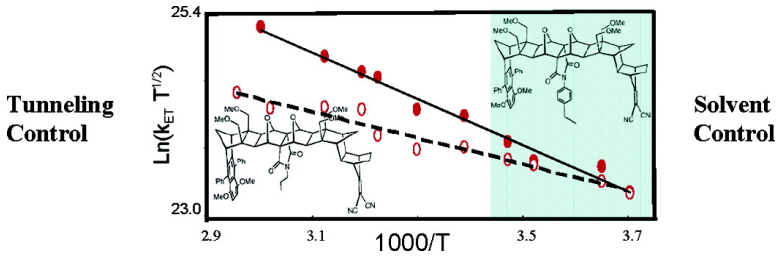

More About This Article

Additional resources and features associated with this article are available within the HTML version:

- Supporting Information
- Links to the 7 articles that cite this article, as of the time of this article download
- Access to high resolution figures
- Links to articles and content related to this article
- Copyright permission to reproduce figures and/or text from this article

View the Full Text HTML

J|A|C|S
ARTICLES
Published on Web 08/06/2004

Observation of Dynamic Solvent Effect for Electron Tunneling in U-Shaped Molecules

Min Liu,[†] David H. Waldeck,*[,†] Anna M. Oliver,[‡] Nicholas J. Head,[‡] and Michael N. Paddon-Row*[,‡]

Contribution from the Chemistry Department, University of Pittsburgh, Pittsburgh, Pennsylvania 15260, and School of Chemistry, University of New South Wales, Sydney, NSW 2052, Australia

Received January 26, 2004; E-mail: dave@pitt.edu; M.PaddonRow@unsw.edu.au

Abstract: The electron-transfer rate constant is measured in two U-shaped donor−bridge−acceptor molecules over a wide range of temperature in acetonitrile and *N*-methylacetamide (NMA). The electron-transfer rate at high temperature can be well described by a nonadiabatic model of the reaction, but at low temperatures the rate in NMA becomes controlled by the solvent. The results are discussed in terms of theoretical models for the change in reaction mechanism and its dependence on the solute−solvent frictional coupling.

Introduction

This work explores rates of intramolecular electron transfer in which the electron tunnels through nonbonded contacts between the electron donor and electron acceptor moieties. Tunneling pathways through nonbonded contacts are important for many bimolecular electron-transfer reactions in biology and chemistry. The electron transfer is studied as a function of solvent and temperature to elucidate how the mechanism changes from a nonadiabatic electron tunneling behavior to a solvent-controlled behavior and to explore how nuclear motion can change the reaction dynamics.

Electron transfer proceeds from a photoexcited dimethoxydiphenylnaphthalene moiety (the electron donor) to a dicyanovinyl moiety (the electron acceptor) in the U-shaped donor−bridge−acceptor (DBA) molecules **1** and **2** (see Figure 1). In our earlier work, the electron transfer was measured over the temperature range of 273−343 K in five different organic solvents and was well-described by a nonadiabatic electron-transfer mechanism.[1,2] In the nonadiabatic limit, the semiclassical rate expression[3]

$$k_{ET} = \frac{4\pi^2}{h}|V|^2 \frac{1}{\sqrt{4\lambda_o \pi k_B T}} \sum_{n=0}^{\infty} \exp(-S)\left(\frac{S^n}{n!}\right) \times \exp\left[-\frac{(\Delta_r G + \lambda_o + nh\nu)^2}{4\lambda_o k_B T}\right] \quad (1)$$

was used to describe the electron-transfer rate of **1** and **2** in different solvents at different temperatures. Five parameters—the reaction free energy, $\Delta_r G$; the solvent reorganization energy, λ_o; an effective vibrational frequency, ν; the electronic coupling, $|V|$; and the Huang−Rhys parameter, S (defined as $S = \lambda_\nu/h\nu$, where λ_ν is the inner reorganization energy)—were quantified through a combination of experimental measurements and modeling. The earlier work quantified these parameters for **1** and **2** at higher temperatures and showed that the solvent effects are only static; that is, the solvent affects the free energies and the energies of activation but does not participate in the important tunneling pathway(s) between the reactant state and the charge-separated state.[4] The molecular solvation model proposed by Matyushov[5] was shown to account for the observed free energy changes quite well. Last, that study showed that the electron tunnels through the pendant moiety (either the 4-ethylphenyl or the propyl group), which lies in the "line-of-sight" between the donor and acceptor groups. The electronic couplings extracted from that analysis were $|V| = 168$ cm^{-1} for **1** and $|V| = 46$ cm^{-1} for **2**, demonstrating that the aromatic pendant group in **1** mediates the electronic tunneling more effectively than the alkyl group in **2**.

The electronic coupling values extracted from this analysis suggest that the electron-transfer mechanism can be manipulated by changing the temperature. This study extends the earlier work to low temperatures to probe the transition from a nonadiabatic electron-transfer mechanism (where the rate is controlled by electron tunneling) to a mechanism in which the rate is controlled by nuclear motion, vide infra. The electron transfer is compared in two solvents, *N*-methylacetamide (NMA) and acetonitrile, as a function of temperature. These solvents have very similar indices of refraction and molecular sizes but dramatically different solvation relaxation times and static

[†] University of Pittsburgh.
[‡] University of New South Wales.

(1) Napper, A. M.; Head N. J.; Oliver A. M.; Shephard, M. J.; Paddon-Row, M. N.; Read, I.; Waldeck, D. H. *J. Am. Chem. Soc.* **2002**, *124*, 10171.
(2) Napper, A M.; Read, I.; Waldeck, D. H.; Head, N. J.; Oliver, A. M.; Paddon-Row, M. N. *J. Am. Chem. Soc.* **2000**, *122*, 5220.
(3) (a) Jortner, J. *J. Chem. Phys* **1976**, *64*, 4860. (b) Barbara, P. F.; Meyer, T. J.; Ratner, M. A. *J. Phys. Chem.* **1996**, *100*, 13148.
(4) Waldeck, D. H.; Zimmt, M. B. *J. Phys. Chem. B* **2003**, *107*, 3580.
(5) Matyushov, D. V.; Voth, G. A. *J. Chem. Phys.* **1999**, *111*, 3630.

10.1021/ja049539d CCC: $27.50

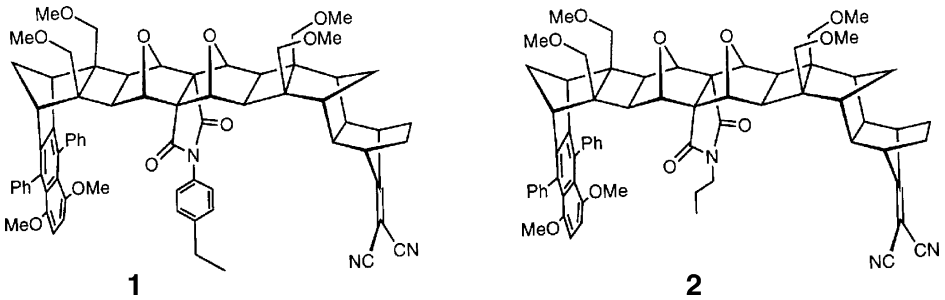

Figure 1. Two U-shaped donor−bridge−acceptor molecules.

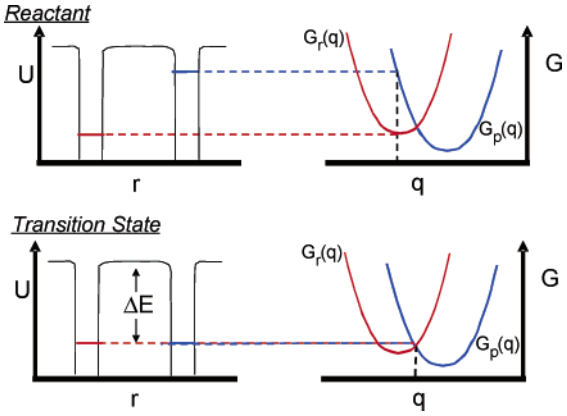

Figure 2. Energetics relevant to electron-transfer reactions for the reactant state (top panel) and the transition state (bottom panel). Both electronic (r) and nuclear (q) coordinates are involved in the reaction.

dielectric constants.[6,7] This difference allows us to explore the effect of solvent nuclear motion on the electron-transfer rate constant.

The observations show that the electron-transfer rate for **1** is significantly faster than that for **2** at room temperature and higher temperatures, consistent with a nonadiabatic electron-transfer process and more efficient electron tunneling via the aromatic pendant group. Upon lowering the temperature to 200 K, the electron-transfer rates for **1** and **2** in NMA become similar; i.e., **1** is not much faster than **2**, demonstrating that the electron transfer is controlled by the environment, not the tunneling pathway. In contrast, the rate constant in acetonitrile remains controlled by the tunneling. The Debye relaxation time of NMA is 390 ps at 303 K[6] but increases dramatically as the temperature decreases, to 13 μs at 201 K, where it is much slower than the electron-transfer reaction.[8] In this limit, the electron-transfer reaction may be controlled by the relaxation time of solvent, a dynamic solvent effect. This effect is manifest by the similar electron-transfer time constants of **1** and **2** at low temperatures, in contrast to their different rate constants at high temperature. These observations demonstrate that the electron-transfer mechanism changes with temperature in NMA.

Electron-Transfer Mechanisms and the Transition between Regimes

Figure 2 illustrates essential features of the generally accepted view of electron-transfer reactions. The electronic energy is sketched as a function of the electron coordinate (on the left) and the nuclear coordinate (on the right); each is approximated as an effective one-dimensional coordinate. The top panel shows the reactant state, the bottom of the Marcus free energy well, for which the electronic energy of the reactant is lower than that of the product and reaction does not occur. The bottom panel shows the nuclear coordinate that corresponds to the transition state, for which the electronic energies are degenerate and the electron can tunnel along the electron coordinate (diagram on the left) between the reactant and product wells. This description of the reaction corresponds to the Franck−Condon approximation, in which the electronic coupling does not depend on the nuclear coordinate but is purely electronic.

Figure 2 underscores the view that a successful electron-transfer reaction requires two things to happen: the nuclear coordinate(s) must evolve to the transition state and the electronic coordinate must change from the reactant to the product. The traditional Marcus theory considers two limits for the reaction rate: nonadiabatic and adiabatic. In the nonadiabatic picture the electronic interaction between the product and reactant curves at the transition state is "weak", and the electron-transfer rate is limited by the electronic motion (probability of tunneling from the reactant to product states). In the adiabatic picture the electronic interaction between the product and reactant curves at the transition state is "strong", and the electron-transfer rate is limited by the nuclear motion to reach the transition state. This traditional view of the reaction does not include the effect of solvent dynamics on either the motion along the nuclear coordinate, in the adiabatic case, or the motion along the electron tunneling pathway, in the nonadiabatic case. Earlier work showed that the solvent does not participate in the electron tunneling pathway for these molecules,[2] so here we restrict the discussion to the solvent's role in effecting the motion along the nuclear reaction coordinate to the transition state.

The important role of solvent dynamics on electron-transfer reactions was first discussed by Zusman.[9] Since that time, a number of workers have addressed this problem.[10−12] The solvent's role in the reaction mechanism can be elucidated through a consideration of time scales for the molecular dynamics in the transition-state region. In the nonadiabatic limit,

(6) Maroncelli, M. *J. Mol. Liq.* **1993**, *57*, 1.
(7) (a) Chapman, C. F.; Fee, R. S.; Maroncelli, M. *J. Phys. Chem.* **1990**, *94*, 4929. (b) Castner, E. W.; Maroncelli, M. *J. Mol. Liq.* **1998**, *77* 1.
(8) a) Kojima, T.; Kawabe, K. *Technol. Rep. Osaka Univ.* **1973**, *23*, 187. (b) Kojima, T.; Kawabe, K. *Oyo Butsuri* **1973**, *42*, 9.
(9) (a) Zusman, L. D. *Chem. Phys.* **1980**, *49*, 295. (b) Zusman, L. D. *Z. Phys. Chem.* **1994**, *186*, 1.
(10) (a) Calef, D. F.; Wolynes, P. G. *J. Phys. Chem.* **1983**, *87*, 3387. (b) Rips, I.; Jortner, J. *Chem. Phys. Lett.* **1987**, *133*, 411.
(11) (a) Sumi, H.; Marcus, R. A. *J. Chem. Phys* **1986**, *84*, 4272. (b) Sumi, H.; Marcus, R. A. *J. Chem. Phys* **1986**, *84*, 4894. (c) Marcus, R. A.; Sumi, H. *J. Electroanal. Chem.* **1986**, *204*, 59. (d) Sumi, H. In *Electron Transfer in Chemistry*; Balzani, V. Ed; Wiley-VCH: New York, 2001; Vol. 1, p 64.
(12) (a) Onuchic, J. N. *J. Chem. Phys.* **1987**, *86*, 3925. (b) Tanimura, Y.; Leite, B. P.; Onuchic, J. N. *J. Chem. Phys.* **2002**, *117*, 2172. (c) Onuchic, J. N.; Beratan, D. N.; Hopfield, J. J. *J. Phys. Chem.* **1986**, *90*, 3707.

the system moves through the transition-state region along the nuclear coordinate many times before a transition occurs from the reactant electronic state to the product electronic state. Hence, the rate-limiting step is the electronic tunneling, not the nuclear motion. In the friction (or adiabatic) limit, the electronic transition from the reactant state to the product state occurs more rapidly than the nuclear motion through the transition-state region because the nuclear motion is slowed by frictional coupling to the environment (or because the electronic coupling is large).

Zusman and others have derived conditions for assessing whether the electron transfer lies in the solvent friction regime. The conditions change somewhat, depending on details of the model and shape of the energy surface in the transition-state region, but they have the same basic features. When a single effective quantized mode contributes to the reorganization, Zusman[9b] finds that the solvent controlled limit applies if

$$\frac{\pi^2|V|^2\tau}{\hbar\lambda_o}\exp\left(-\frac{\lambda_v}{h\nu}\right) \gg \sin\left(\frac{\pi}{2}\left(\frac{\Delta_r G}{\lambda_o}+1\right)\right) \qquad (2)$$

in which τ is a characteristic solvent relaxation time. If $|\Delta_r G| \ll \lambda_0$ and one combines the internal reorganization energy term with the electronic coupling to define an effective electronic coupling $|V_{eff}|$,[13] the inequality 2 reduces to a form like that found by Onuchic,[12] namely

$$g = \frac{|V_{eff}|^2\tau}{\hbar\lambda_o} \gg 1 \qquad (3)$$

The adiabaticity parameter g compares the characteristic time required for electron tunneling to the characteristic time spent in the transition-state (Landau−Zener) region. The reaction is adiabatic when $g \gg 1$, and it is nonadiabatic when $g \ll 1$. If these criteria are applied using the parameters in Table 3, $\tau \gg$ 5 ps for **1**, and $\tau \gg 30$ ps for **2**.

The observed electron-transfer rate is often described by an interpolation formula that connects the nonadiabatic and solvent-controlled (adiabatic) limits, namely

$$\frac{1}{k_{ET}} = \frac{1}{k_{NA}} + \frac{1}{k_{SC}} \qquad (4)$$

where k_{NA} is the nonadiabatic rate constant, k_{SC} is the rate constant in the solvent-controlled limit, and k_{ET} is the measured electron-transfer rate. Equation 4 results because both an electronic state change (rate-limiting for k_{NA}) and nuclear motion to the transition state (rate-limiting for k_{SC}) must occur for reaction; hence, the slower process is rate controlling. Although eq 4 provides a way to interpolate between the two limiting behaviors, it does not describe the dynamics of the reaction accurately. For example, the rate is exponential in the nonadiabatic regime but can be nonexponential in intermediate regimes. More dramatically, if the solute−solvent frictional coupling is strong and slow, the reaction trajectory will not go through the transition state. Rather it may occur at a range of different polarization coordinates.[11,14]

(13) In this case $|V_{eff}| = \sqrt{\pi}|V|\exp(-\lambda_v/2h\nu)$.
(14) (a) Berezhkovskii, A. M.; Zitserman, V. Y. *Physica A* **1990**, *166*, 585. (b) Berezhkovskii, A. M.; Zitserman, V. Y. *Chem. Phys. Lett.* **1990**, *172*, 235. (c) Waldeck, D. H. *J. Mol. Liq.* **1993**, *57*, 127.

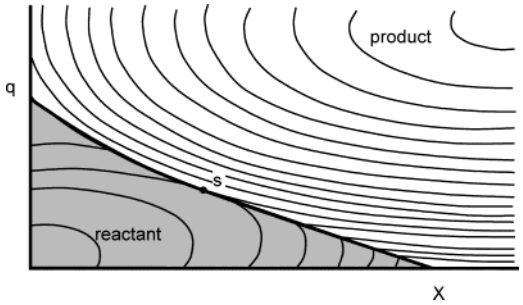

Figure 3. Two-dimensional $V(q,X)$ reaction coordinate. The shaded area represents the reactant surface. The thick line is the dividing line (ridge) between the reactant and product surfaces. The reactant well is at the bottom left, the product well is at the top right, and point S is the saddle point on the ridge line. Adapted from ref 11.

The Sumi−Marcus model of electron transfer explicitly includes solvent dynamics by viewing the reaction as proceeding along a two-dimensional effective potential energy surface, $V(q,X)$ (see Figure 3). The coordinate q in this reaction surface corresponds to the typical reaction coordinate used in electron-transfer reactions (Figure 2, right-hand panels) and includes internal and low-frequency nuclear degrees of freedom that are always "fast". The second coordinate, X, is the solvent polarization coordinate, i.e., an effective coordinate that accounts for the polarization response of the medium to the evolving charge distribution of the reactant. Sumi and Marcus[11] find the reaction rate by solving a Fokker−Planck equation for diffusive motion along X and treat the motion along q through a rate constant $k(X)$ which is X dependent and depends on the "fast" motions in the normal way (e.g., eq 1). In particular, they solve

$$\frac{\partial P(X,t)}{\partial t} = D\frac{\partial^2 P(X,t)}{\partial X^2} + \frac{D}{k_B T}\frac{\partial}{\partial X}\left(P(X,t)\frac{dV(X)}{dX}\right) - k(X)P(X,t) \qquad (5)$$

where D is the diffusion coefficient, $V(X)$ is the effective potential for the polarization coordinate, and $P(X,t)$ is a probability distribution function for the reactant, i.e., the concentration. This model treats the time evolution of the reactant probability by diffusion along the X coordinate (the first two terms describe diffusion in a potential) and its first-order decay at the different X values ($k(X)$ acts as a loss term for the probability). The time-dependent behavior of $P(X,t)$ should be reflected by the reactant's time evolution in an experiment.

Sumi and Marcus discuss four limiting cases for the reaction. They call the first case the "slow reaction limit". It corresponds to motion along X that is fast compared to the motion along q, so that the traditional analysis applies (be it nonadiabatic or adiabatic) and the reaction does not depend on solvent frictional coupling. This case applies for the high-temperature data (see Figure 6). Their second case is called the "wide reaction window". It corresponds to a situation in which the internal reorganization energy is much larger than the solvent reorganization, so that the reaction may proceed at a range of X values but the reaction rate at each of the different X values is the same. Their third ("narrow reaction window") and fourth ("nondiffusing limit") cases may be relevant to the low-temperature experiments reported here. Both of these latter cases predict a nonexponential decay of the reactant population

because the motion along the polarization coordinate is slow compared to the reaction rate.

In the "narrow reaction window" case, Sumi and Marcus assume the electron transfer occurs at a particular value of $X = X_0$ and the nonexponentiality arises from the time evolution of the reactant population along X. This limit corresponds to motion in X being slow, so that the time behavior is determined by diffusion along X to the position X_0 where the electron transfer occurs, given by a "sink" term in the reaction diffusion equation. Hence, the reaction coordinate is X and effectively one-dimensional. This limit of the model is useful for understanding dynamic Stokes shift experiments, in which the optical excitation and emission can be viewed as an electron-transfer reaction within the chromophore.[6,15]

In the "nondiffusing limit", the motion along X is frozen and the electron transfer occurs at a range of X values so that the nonexponentiality reflects the dispersion in $k(X)$. This limit is quite different from the traditional view of the reaction proceeding through a well-defined transition state. In this case, a range of reaction trajectories are possible and the choice of which to follow is determined dynamically by the medium's polarization response. This limit requires a description with at least two dimensions.

Experimental Section

The synthesis of the U-shaped supermolecules is similar to that reported earlier;[16] however, the detailed procedure is included in the Supporting Information. The solvent acetonitrile (99.9% HPLC) was purchased from Burdick & Jackson. *N*-Methylacetamide (NMA) was purchased from Aldrich and was fractionally distilled three times using a Vigreux column under vacuum. The purified fraction was used immediately in all the experiments. Each solution was freeze−pump−thawed a minimum of five times to eliminate dissolved gases.

In our experiment, the sample was excited at 310 nm by the frequency-doubled cavity-dumped output of a Coherent CR599-01 dye laser, using Rhodamine 6G dye, which was pumped by a mode-locked Coherent Antares Nd:YAG. The dye laser pulse train had a repetition rate of ca. 300 kHz. Pulse energies were kept below 1 nJ, and the count rates were kept below 3 kHz to prevent pile-up effects. All fluorescence measurements were made at the magic angle, and data were collected until a standard maximum count of 10 000 was observed at one channel.

Time-resolved fluorescence kinetics of **1** and **2** and their donor-only analogues were measured in acetonitrile and NMA as a function of temperature. The lowest temperature was 200 K and the highest was 338 K. The experimental temperature was controlled by an ENDOCAL RTE-4 chiller in the high-temperature range, and the temperature was measured using a Type-K thermocouple (Fisher-Scientific), accurate to within 0.1 °C. The low-temperature experiments were carried out in a VPF-100 Cryostat (Janis Research Co., Inc.) and were operated with a 2×10^{-5} Torr high vacuum during the experiment. The low-temperature instrumental setup is shown in the Supporting Information (Figure S1). For the low-temperature experiments, the temperature was measured using a model 321 autotuning temperature controller (LakeShore Cryotronics, Inc.) which has a silicon diode, accurate to within 0.1 K.

The instrument response function was measured using a sample of colloidal $BaSO_4$. Samples **1** and **2** each contain a small amount of unreacted donor compound. Independent experiments on the donor-only molecules were used to characterize the donor's single-exponential fluorescence decay, which is much longer than the relaxation time of **1** and **2** at the measured temperatures. The contribution of the donor-only impurity was removed from the fluorescence decay curves for **1** and **2** in the analysis.[17] The remaining parts of the **1** and **2** decay laws were fit to either one or two exponentials using IBH-DAS6 analysis software. Other fitting and data presentation, e.g., eq 1, was performed using Microsoft Excel XP.

Table 1. Properties of Solvents Acetonitrile (ACN) and NMA at 303 K

solvent	refractive index	static dielectric constant	Debye relaxation time (ps)	density (g/mL)	viscosity (cP)	dipole moment (D)
ACN	1.341	34.75	3	0.7696	0.331	3.48
NMA	1.429	178.9	390	0.9503	3.885	5.05[a]

[a] Calculated using Gaussian/MP2/6-31G.

The current work measures the electron-transfer kinetics for systems **1** and **2** in acetonitrile and NMA solvents and combines them with earlier data obtained in polar solvents CH_2Cl_2, tetrahydrofuran, and acetonitrile and the weakly polar solvents toluene and mesitylene.[2] Some properties of NMA and acetonitrile solvents are listed in Table 1. NMA has a freezing point of 302 K and allows access to very slow polarization response times for the solvent.[6,8] Electron-transfer rate studies in organic solids have been performed previously by other groups and provide no extraordinary technical difficulties.[18] No unusual features in the reaction kinetics are observed in the region of the freezing point.

Results

The intramolecular photoinduced electron transfer in **1** and **2** occurs from the locally excited singlet state of the dimethoxydiphenylnaphthalene donor to the dicyanovinyl acceptor. By comparing the fluorescence decay rates of the supermolecule with and without the electron acceptor group, it is possible to determine the electron-transfer rate.[1]

Fluorescence Decay. Figure 4 presents some representative fluorescence decay curves for **1** in acetonitrile (panel A) and in NMA (panel B), and Table 2 presents the corresponding fitting parameters for these decay curves. The fluorescence decay law in acetonitrile is single exponential over the entire temperature range. In this case the fluorescence decay rate constant k_f can be used to determine the electron-transfer rate constant k_{ET}. The electron-transfer rate constant is given by $k_{ET} = k_f - k_{donor\ only}$, where $k_{donor\ only}$ is the fluorescence decay constant determined for the analogue molecule without an electron acceptor and provides a good measure of the locally excited state's intrinsic decay rate.

The fluorescence decay law for **1** in NMA is nonexponential (see Figure 4B); hence, a single rate constant does not fully describe the data. Table 2 shows parameters for a double-exponential fit, and it is evident that the rate law becomes more exponential as the temperature increases. In fact, a fit of the fluorescence decay at 313 K has a fast time constant that comprises 94% of the overall decay law. To quantify these data, we compute the correlation time τ_c for the decay (see Table 2). The fluorescence decay data for **2** show a trend similar to those

(15) (a) Maroncelli, M.; MacInnis, J.; Fleming, G. R. *Science* **1989**, *243*, 1674. (b) Barbara, P. F.; Walker, G. C.; Smith, T. P. *Science* **1992**, *256*, 975. (c) Castner, E. W.; Bagchi, B.; Fleming, G. R. *Chem. Phys. Lett.* **1988**, *143*, 270. (d)Van der Zwan, G.; Hynes, J. T. *J. Phys. Chem.* **1985**, *89*, 4181. (e) Bagchi, B.; Oxtoby, D. W.; Fleming, G. R. *Chem. Phys.* **1984**, *86*, 257.

(16) Head, N. J.; Oliver, A. M.; Look, K.; Lokan, N. R.; Jones, G. A.; Paddon-Row, M. N. *Angew. Chem., Int. Ed.* **1999**, *38*, 3219.

(17) The molecular structures for the donor-only compounds may be found in ref 1.

(18) (a) Gaines, G. L., III; O'Neil, M. P.; Svec. W. A.; Niemczyk, M. P.; Wasielewski, M. R. *J. Am. Chem. Soc.* **1991**, *113*, 719. (b) Miller, J. R. *Science* **1975**, *189*, 221.

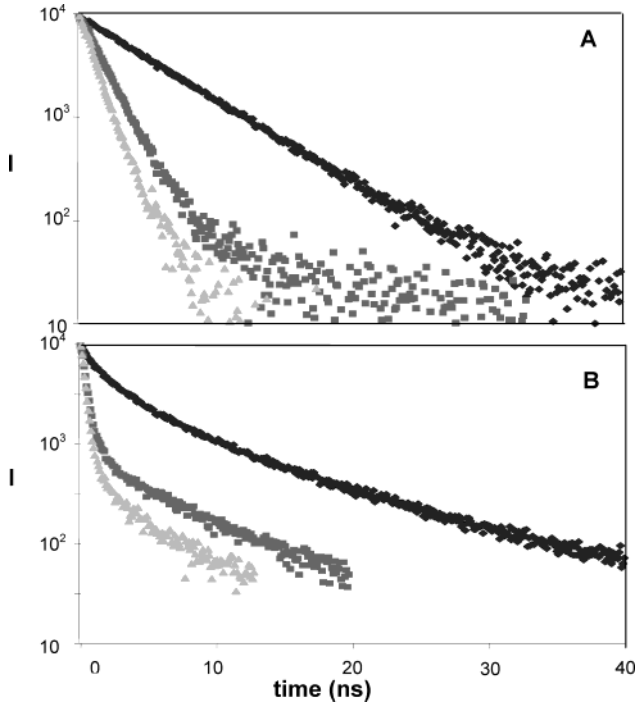

Figure 4. Fluorescence decay profiles for **1** in acetonitrile (panel A) at (diamonds) 200 K, (squares) 295 K, and (triangles) 321 K and in NMA (panel B) at (diamonds) 200 K, (squares) 295 K, and (triangles) 313 K.

Table 2. Fitting Parameters for the Fluorescence Decays in Figure 4

	T, K	τ_1 (%), ns[a]	τ_c, ns[b]		*T*, K	τ_1 (%), ns[a]	τ_c, ns[b]
1 in NMA	200	1.64 (74)	3.06	**2** in NMA	200	2.41 (79)	4.12
1 in NMA	295	0.40 (93)	0.49	**2** in NMA	295	0.67 (97)	0.68
1 in NMA	313	0.27 (94)	0.30	**2** in NMA	313	0.46 (98)	0.46

[a] τ_1 is the fast time constant and % is its percentage contribution to the total decay curve. [b] $\tau_c = \sum A_i\tau_i$, where A_i is the percentage of component *i* and τ_i is the decay time for component *i*, in a fit of the decay law to a sum of exponentials.

found for **1**, except that the nonexponentiality is not as pronounced (see Supporting Information).

To summarize, the decay law in acetonitrile is well described by a single exponential over the whole temperature range, and the decay law in NMA is well described by a single exponential at high temperatures (above 300 K) but is strongly nonexponential at low temperatures (below 290 K).

Steady-State Spectra. An important difference between NMA and acetonitrile arises from hydrogen-bonding. The hydrogen-bonded structures in NMA are largely responsible for the large dielectric constant and slow polarization relaxation of the solvent.[7,8,19] Figure 5 shows the steady-state absorption and fluorescence spectra of **1** in acetonitrile and NMA at room temperature. It is evident that the spectral characteristics are very similar in the two solvents. These observations suggest that any difference in the interaction between the solute and the solvents, acetonitrile and NMA, does not involve any significant perturbation of the donor chromophore.

Data Analysis

High-Temperature Results. At high temperatures (>302 K) the rate law in NMA becomes nearly exponential. The worst-case scenario is **1** in NMA at 305 K, for which the calculated correlation time is 392 ps and the fast decay time in a double-exponential fit is 334 ps, about a 15% difference. As the temperature increases, the correspondence between the correlation time and the fast decay component improves. Although not rigorous, it is reasonable to approximate the decay law as single exponential in this regime.

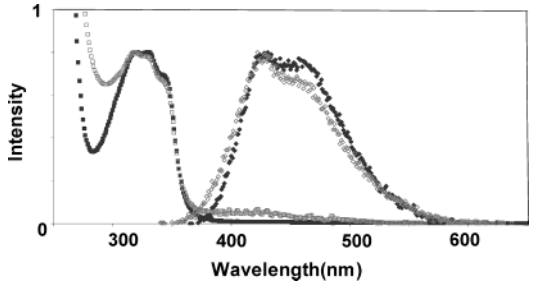

Figure 5. Absorption (squares) and fluorescence (diamonds) spectra for **1** in NMA (gray) and acetonitrile (black).

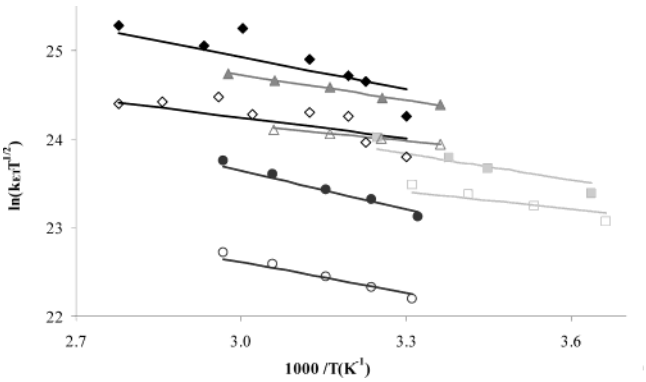

Figure 6. Fitting electron-transfer rate of **1** (filled symbols) and **2** (open symbols) in different solvents at high temperature: (diamonds) NMA, (triangles) tetrahydrofuran, (squares) dichloromethane, and (circles) acetonitrile.

The previous work in our group fit the temperature dependence of the experimental rate constant to the semiclassical equation and obtained the electronic coupling $|V|$ and solvent reorganization energy λ_o values. The reaction free energy $\Delta_r G$ was determined from experimental fluorescence lifetime data in weakly polar and nonpolar solvents, from which the forward electron-transfer rate and backward rate can both be determined. Electronic structure calculations and the experimental free energies of reaction in the aromatic solvents[4] were used to calibrate a molecular solvation model and determine the values of parameters in the semiclassical electron-transfer expression.

Figure 6 combines those earlier data with these new data for **1** and **2** in NMA and acetonitrile at high temperatures (>300 K). When calibrated to the measured free energies in nonpolar solvents, the molecular solvation model and the semiclassical equation (eq 1) provide a good representation of the data. This finding supports the identification of nonadiabatic electron transfer for the high-temperature mechanism, even in NMA. The experimental electron-transfer rate constant of **1** is about 1.7 times faster than that for **2** in NMA, which matches well with the previous conclusion that the aromatic group is better than an alkyl group at mediating the electronic coupling. The fitting was performed in the same manner described previously.[1] Because more data are included in the fit, the best-fit parameters changed slightly (see Table 3). The electronic coupling value

(19) Knecht, L. A. *Pure Appl. Chem.* **1971**, *27*, 281.

Table 3: Fitting Parameters for **1** and **2** to the Nonadiabatic Model at High Temperature[a]

		CH_3CN		NMA	
system	$\|V\|$, cm^{-1}	λ_o, eV	Δ_rG, eV	λ_o, eV	Δ_rG, eV
1	146	1.48	−0.54	1.03	−0.35
2	62	1.46	−0.58	1.01	−0.39

[a] $\lambda_v = 0.63$ eV and $h\nu = 1600$ cm^{-1} are determined from charge-transfer spectra of related species (see ref 1).

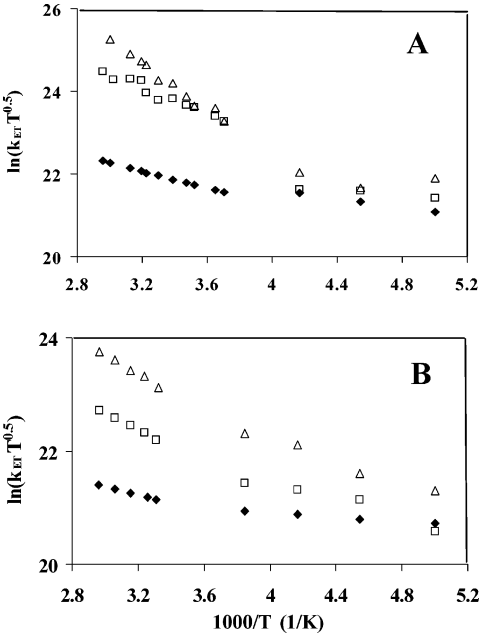

Figure 7. Experimental rate constants of **1** (open triangle), **2** (open square), and the donor-only compound (filled diamond) as a function of temperature in NMA (panel A) and in acetonitrile (panel B).

for **1** is 146 cm^{-1}, and that for **2** is 62 cm^{-1}, which is consistent with the earlier analysis.

Low-Temperature Results. Figure 7A presents the experimental data in NMA over the temperature range from 200 to 338 K. The electron-transfer rates of **1** and **2** are plotted versus 1000/*T*, and the fluorescence decay rate of the donor-only molecule is plotted versus 1000/*T*, as well. This plot illustrates the different electron-transfer rate constants for **1** and **2** at temperatures higher than 300 K and their similar rate constants at lower temperatures, down to 200 K. For temperatures below 200 K, the electron transfer appears to be frozen out and the fluorescence decays of **1** and **2** coincide with that of the donor-only compound.

These data do not determine whether the rate law is controlled by the solvent or by internal dynamics of the molecule. These two possibilities were analyzed by studying the electron transfer in a solvent which has a very fast relaxation time, acetonitrile. Figure 7B shows the rate data for **1** and **2** in acetonitrile over the entire temperature range along with the fluorescence decay rate data for the donor-only compound. The plot shows that the electron-transfer rates of **1** and **2** remain separated even as the temperature approaches 200 K. Since the rate constants are still quite different in acetonitrile, this finding demonstrates that temperature alone is not the controlling factor for the behavior in NMA.

The major difference between acetonitrile and NMA is the solvent polarization relaxation time. For acetonitrile it is 3.2 ps[6] at 298 K, which is about 100 times faster than that for NMA. As the acetonitrile is cooled, its relaxation time increases but is still much faster than that of NMA at room temperature. Hence, the solvent dynamics does not affect the observed electron-transfer rate, even at these low temperatures. In short, the electron-transfer rate in acetonitrile follows the same trend at low temperature (295−200 K) as at high temperatures (>295 K) and is well-described as nonadiabatic.

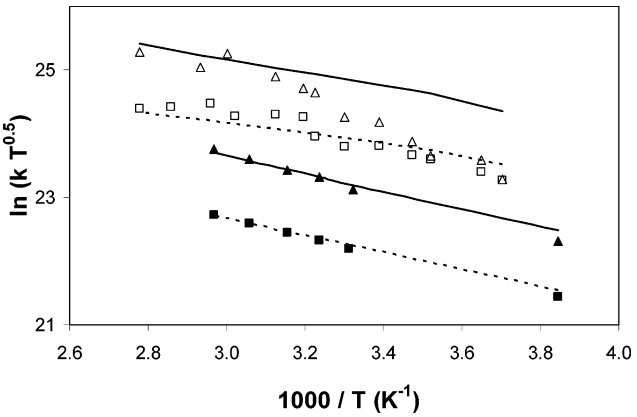

Figure 8. Plots of the electron-transfer rate constant versus 1000/*T* for **1** (triangles) and **2** (squares) in NMA (open symbols) and acetonitrile (filled symbols). Straight and dashed lines are fits to eq 1.

Mechanism Change. The difference in behavior for the electron-transfer rate constant in NMA, compared to that in acetonitrile, implies a change in reaction mechanism that is linked to the slow relaxation dynamics of the NMA solvent. The Sumi−Marcus model can explain this behavior as a transition from the "slow reaction" limit at high temperature to one of the solvent friction limiting cases at low temperature. In the "nondiffusing limit" the reaction rate is inhomogeneous, and the observed rate behavior depends on the initially prepared distribution of the reactant along *X*. Although no dramatic dependence of the preparation is observed for small changes in the excitation conditions, more extensive studies of this sort need to be examined before this limit can be discounted. For the "narrow reaction window" limit, the dynamics along the solvent coordinate controls the reaction rate. We analyze the implications of this limit for the data and discuss what motion may influence the behavior.

The transition from the "slow reaction" limit to the "narrow reaction window" limit can be approximated by the interpolation formula, eq 4, for the change in reaction mechanism. This approximation provides a way to extract the rate constant k_{SC} for the solvent-controlled rate process when the nonadiabatic rate constant is known. Because the electron-transfer reaction for **1** and **2** in acetonitrile appears to follow a nonadiabatic mechanism over the entire temperature range, these data can be used to determine the displacement in the rate constant magnitudes which arises from the different electronic couplings. If the rate constant for **2** in NMA is assumed to be nonadiabatic over the entire temperature range, then the electronic coupling ratio between **2** and **1** can be used to predict what the nonadiabatic rate constant should be for **1** in NMA.

Figure 8 plots the $\ln(k_{ET}\sqrt{T})$ of **1** and **2** in acetonitrile and NMA versus 1000/*T*. The acetonitrile data are fit to the semiclassical expression (eq 1), with the parameters obtained from fitting the data in Figure 6. Because the NMA solidifies

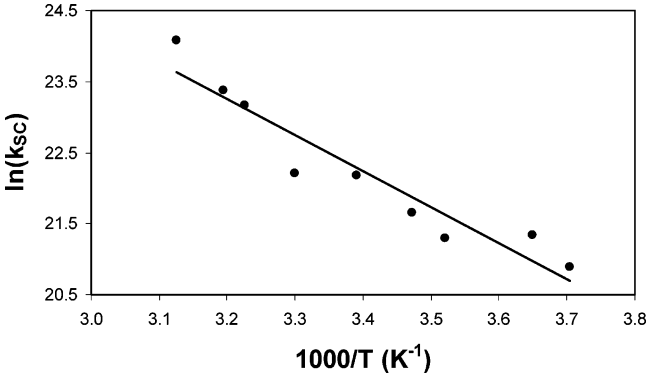

Figure 9. Arrhenius plot for the rate constant k_{SC}. See text for details.

below 303 K, the molecular solvation model was not used to determine the solvent reorganization and solute free energy. Instead, the rate data for **2** in NMA are fit to eq 1 with the solvent reorganization and reaction free energy determined by a dielectric continuum model, while the internal reorganization and electronic coupling parameters are fixed at the values obtained from the high-temperature fits. Table 3 gives the free energy and reorganization parameters for NMA at high temperature. Taking the offset in electronic coupling and reaction free energy from the fit to the high-temperature data in Figure 6, the fit for **2** in NMA was used to predict a nonadiabatic rate constant for **1** in NMA (upper curve in Figure 8).

Using this predicted nonadiabatic rate constant, the solvent-controlled rate constant of **1** in NMA can be calculated. Figure 9 plots the $\ln(k_{SC})$, obtained in this manner, versus $1000/T$. The plot shows that the rate constant increases as the temperature increases, and the slope gives an activation energy of 42 kJ/mol. Although data are not available for the solvation dynamics of NMA solid, temperature-dependent measurements of NMA's dielectric relaxation time over the range of 201−227 K give an activation enthalpy of 84 kJ/mol (70 kJ/mol for the longitudinal relaxation time). If the solvent's dielectric relaxation is linked to the electron-transfer reaction, the disparity in the activation barriers suggests that the frictional coupling may not lie fully in the Smoluchowski limit; i.e., the rate constant is not inversely proportional to the polarization relaxation time. In this case the coupling would lie in an "intermediate regime" (see refs 11 and 20). This comparison is very suggestive, and experiments to measure the solvation dynamics in NMA, for comparison with these electron-transfer rate constants, are underway.

Phenyl Ring Torsion. An alternative interpretation of the rate constant k_{SC} is conformational gating. This model treats the reaction rate as arising from a conformational rearrangement to an activated state (geometry) from which nonadiabatic electron transfer may occur. A detailed discussion of possible geometrical changes in these electron-transfer systems is available elsewhere.[1] To summarize that discussion, the geometry of the system at which electron transfer occurs is different from the reactant geometry. Extrapolating from the computed relaxed geometry of the charge-separated state, the electron-transfer transition-state structure should differ from the reactant's structure only in the two chromophores being bent toward each other. Those findings indicate that the molecular volume decreases upon reaching the transition state; hence, it is unlikely that this change in geometry would be impeded by solvent in the solid state. Because the cavity has very little free space, it is unlikely that any solvent molecules occupy the cavity, and inward motion of the chromophores would not be impeded. On the other hand, torsion of the phenyl group about the imide N-phenyl bond is another likely motion, and may possibly be coupled to the solvent coordinate.

For this motion to act as a "gate" for the electron transfer, the phenyl torsion must modulate the magnitude of the electronic coupling because of differences in the phenyl ring's interaction with the donor and acceptor groups. Important factors in determining the electronic coupling are the distances between the N-phenyl group and the donor and acceptor groups. A range of distances are available between the wing chromophores and the N-phenyl group, but the closest contacts are 3.8 Å for the naphthalene−N-phenyl distance and 3.9 Å for the DCV−N-phenyl separation. The average distances are about 4.0 Å for the DMN−phenyl and 4.4 Å for the DCV−N-phenyl separation. Hence, there is ample scope for "through-space" orbital interactions between the wing chromophores and the N-phenyl ring. A second important factor is the amount of orbital overlap. Even though a particular conformation may have a somewhat closer distance, the net orbital overlap and electronic coupling can be smaller. To focus the discussion, we compare the magnitude of the electronic coupling for the conformation in which the phenyl ring is nearly coplanar with the imide ring (**1m-coplanar**, Figure 10) to that in which the phenyl ring is perpendicular to the imide ring (**1m-perp**, Figure 10).

On the basis of orbital overlap considerations, the donor-to-acceptor coupling through the π and π^* molecular orbitals of the central phenyl group might be stronger in the coplanar conformation than in the perpendicular one. Indeed, B3LYP/6-31G(d) Koopmans' theorem calculations[21] on the B3LYP/6-31G(d) optimized C_{2v} models **3** (Figure 11) suggest that the electronic coupling for the coplanar conformation, **3-coplanar**, is stronger than that for the perpendicular conformation, **3-perp**. The calculations include all types of orbital interactions; however, the π-orbital interactions make the largest contribution. The electronic coupling was obtained from one-half of the splitting energies for the symmetric structures in Figure 11, in the Koopmans' theorem limit. The HOMO orbital splitting gives an electronic coupling of 40 cm^{-1} in the coplanar geometry and 23 cm^{-1} in the perpendicular geometry. Similarly, the LUMO orbital splitting gives couplings of 38 cm^{-1} in the coplanar geometry and 11 cm^{-1} in the perpendicular geometry.

In light of this finding, it was deemed necessary to compute the N-phenyl rotational barrier, and this was done at the B3LYP/6-31G(d) level of theory using the model system, **1m**, which differs from the experimentally studied one, **1**, by replacement of the four methoxymethylene groups of the latter system by

(20) (a) Waldeck, D. H. *Chem. Rev.* **1991**, *91*, 415. (b) Weaver, M. J. *Chem. Rev.* **1992**, *92*, 463.

(21) All calculations reported in this paper were carried out at the B3LYP/6-31G(d) level of theory using the GAUSSIAN 98 package: Frisch, M. J.; Trucks, G. W.; Schlegel, H. B.; Scuseria, G. E.; Robb, M. A.; Cheeseman, J. R.; Zakrzewski, V. G.; Montgomery, J. A., Jr.; Stratmann, R. E.; Burant, J. C.; Dapprich, S.; Millam, J. M.; Daniels, A. D.; Kudin, K. N.; Strain, M. C.; Farkas, O.; Tomasi, J.; Barone, V.; Cossi, M.; Cammi, R.; Mennucci, B.; Pomelli, C.; Adamo, C.; Clifford, S.; Ochterski, J.; Petersson, G. A.; Ayala, P. Y.; Cui, Q.; Morokuma, K.; Malick, D. K.; Rabuck, A. D.; Raghavachari, K.; Foresman, J. B.; Cioslowski, J.; Ortiz, J. V.; Stefanov, B. B.; Liu, G.; Liashenko, A.; Piskorz, P.; Komaromi, I.; Gomperts, R.; Martin, R. L.; Fox, D. J.; Keith, T.; Al-Laham, M. A.; Peng, C. Y.; Nanayakkara, A.; Gonzalez, C.; Challacombe, M.; Gill, P. M. W.; Johnson, B.; Chen, W.; Wong, M. W.; Andres, J. L.; Gonzalez, C.; Head-Gordon, M.; Replogle, E. S.; Pople, J. A. *Gaussian 98*, Revision A.7; Gaussian Inc: Pittsbugh, PA, 1998.

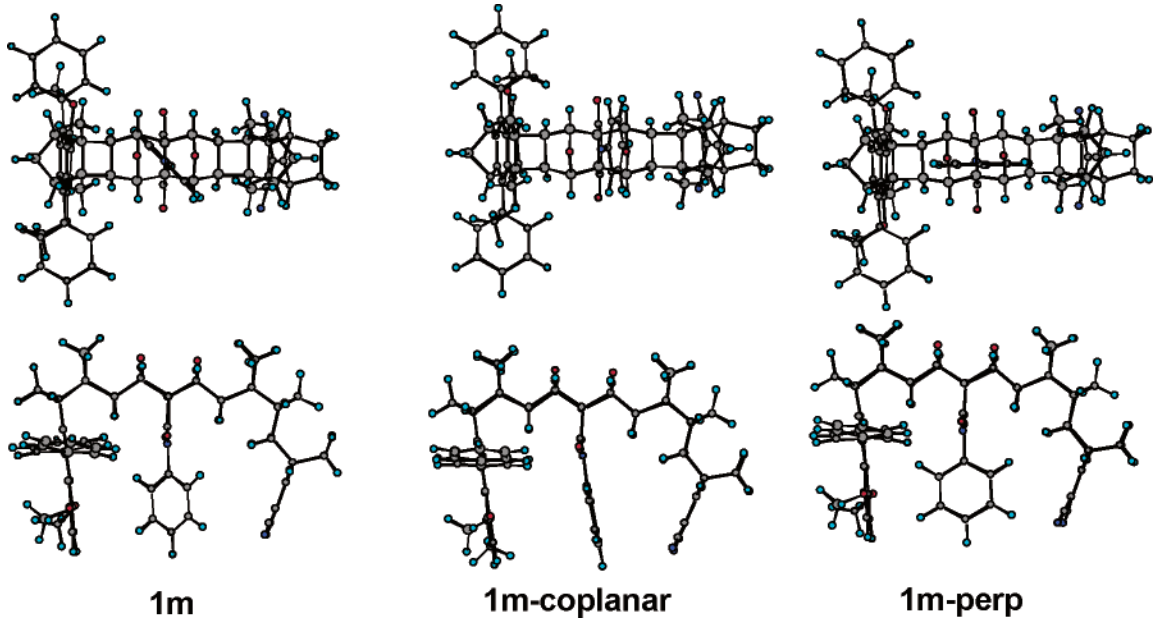

Figure 10. Three optimized B3LYP/6-31G(d) gas-phase structures of **1m**, differing in the conformation of the phenyl ring with respect to the imide group. **1m** differs from **1** only in that the four methoxymethylene groups have been replaced with methyl groups and the ethyl substituent on the phenyl ring has been removed.

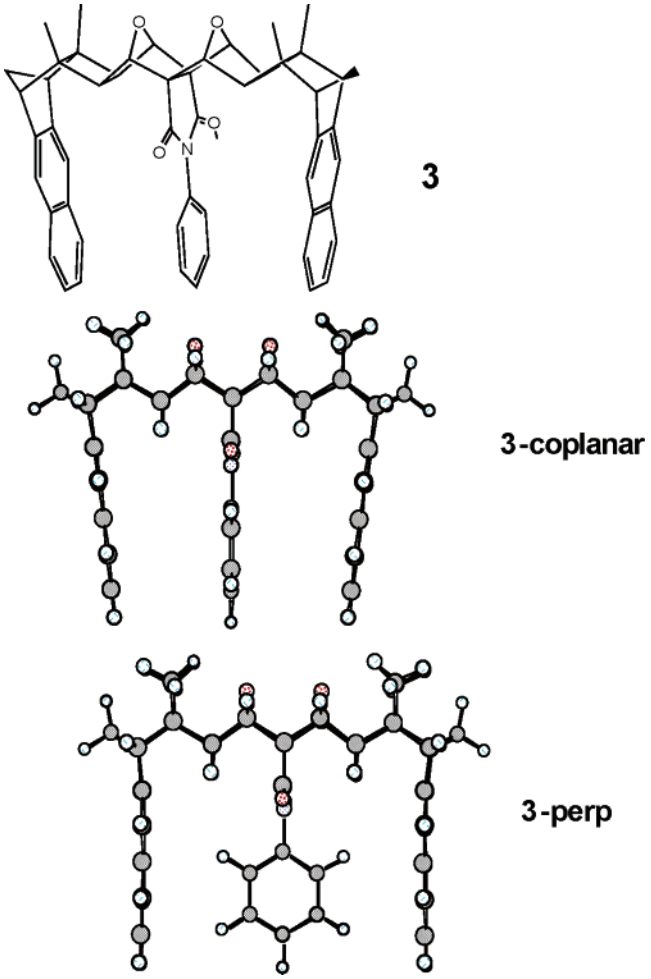

Figure 11. B3LYP/6-31G(d) optimized C_{2v} gas-phase structures, **3-coplanar** and **3-perp**, in which the phenyl ring is respectively coplanar and perpendicular to the imide ring.

methyl groups and by removal of the ethyl substituent from the phenyl ring. All calculations refer to gas-phase structures.[21]

The fully optimized, global minimum energy structure for **1m** has the phenyl ring oriented 43° with respect to the plane of the imide ring. Two distinct rotational barriers for the N-phenyl group may be envisaged, namely with the phenyl ring lying either approximately coplanar with the imide ring or perpendicular to it, and the transition structures corresponding to these rotational barriers were duly located (see **1m-coplanar** and **1m-perp**, Figure 10). Although they were optimized using no symmetry constraints, both optimized structures closely resemble the expected C_s symmetry. Note that for **1m-coplanar**, the phenyl ring actually bends a little out of coplanarity with the imide ring, toward the dicyanovinyl group.

The (vibrationless) rotational barriers, calculated from these structures, are 3.3 kJ/mol for passage through **1m-coplanar** and about 1 kJ/mol or less for the **1m-perp**. These barriers are extremely small and, for all intents and purposes, the phenyl group in **1m** (and **1**) may be regarded as a free rotor. The magnitude of the electronic coupling between the phenyl group and the donor and acceptor chromophores in **1** is a Boltzmann weighted average, determined by the shape of the rotational barrier, of the different phenyl geometries.[4] Given the extreme shallowness of this barrier, it is likely that the magnitude of this coupling will not change significantly over the range of temperatures used in our electron-transfer experiments. Comparison of this small barrier with that obtained from the analysis using eq 4 (vide supra) suggests that the phenyl torsion would need to be strongly coupled to the solvent matrix to act as the rate-controlling step.

Discussion and Conclusion

The experimental observations reveal that the electron transfer for **1** in NMA changes from a nonadiabatic mechanism at high temperatures to a solvent-controlled (or adiabatic) mechanism at low temperatures. This conclusion is supported by two primary observations. First, the observed excited-state decay law changes from a simple exponential in acetonitrile solvent to a nonexponential form in NMA. The nonexponentiality

increases with the coupling strength between the donor and acceptor species (**1** versus **2**) and the increase in the solvent relaxation time. Second, when the reaction rate is characterized by the correlation time of the emission decay law, the rate constant for **1** and **2** changes from being displaced in magnitude at high temperature (because $|V|$ is different) to being the same at low temperature. This change to a rate constant that correlates with the solvent relaxation dynamics (characterized by viscosity or polarization relaxation time) rather than the electronic coupling strength, and the nonexponentiality of the decay law, are both experimental signatures of a change in the reaction mechanism.

Two possible explanations for the change in reaction mechanism are discussed: a transition from nonadiabatic electron transfer to solvent-controlled (adiabatic) electron transfer and conformational gating. A change in the reaction mechanism from nonadiabatic to friction-controlled could arise from the increasing polarization relaxation time of the NMA solvent as it is cooled. Using the model developed by Zusman[9b] (eq 2) and the fitting parameters in Table 2, the electron transfer in NMA and acetonitrile solvents at room temperature will be in the solvent friction limit when the solvent's polarization relaxation time $\tau \gg 30$ ps for **2** and $\tau \gg 5$ ps for **1**. The relaxation time in acetonitrile is significantly faster than this time scale (<1 ps at room temperature[6]), and the electron-transfer rate constant appears to remain nonadiabatic over the entire temperature range. By lowering the temperature and increasing the relaxation time τ in NMA (measured to be 20−40 ps at 300 K[6]), we can move the system strongly into the solvent-controlled regime. Because the polarization relaxation (solvation) time in NMA has not been measured over this temperature range, it is currently not possible to ascertain if the rate constant correlates with the solvent relaxation time in the predicted manner.

An "alternative" explanation for the solvent-dependent electron transfer is the conformational gating mechanism, which has found wide use in protein electron-transfer studies.[22] For example, the torsional motion of the phenyl ring in the cavity can modulate the electronic coupling magnitude. It is possible that other motions, in particular compression of the donor-to-acceptor distance, might play a role and couple to the phenyl torsional motion. The acetonitrile studies show that such motion is not completely frozen out by the low temperatures; however, the large viscosity in NMA may act to hinder this motion and give rise to solvent control. Independent studies of the phenyl torsional dynamics can be used to assess whether this mechanism is operative.

Both the "gating" mechanism and the solvation dynamics controlling the electron-transfer mechanism correspond to the "narrow reaction window" limit of the Sumi−Marcus treatment. In the case of electron transfer controlled by the solvent dynamics, the polarization coordinate X would be interpreted in the manner described by Sumi and Marcus. In the case of conformational gating, the X coordinate should correspond to a conformational (or configurational) change of the reactant, in this case, identified with the phenyl torsional "gate". An advantage of using the Sumi−Marcus description is that the nonexponential character of the reactant's population density is included in a natural way, from the diffusion of the system in the solvent coordinate.

By studying the electron-transfer kinetics of two U-shaped molecules over a wide range of temperature in acetonitrile and NMA, a change in the electron-transfer mechanism is identified. The experimental manifestations of this mechanism change are nonexponential decay laws and rate constants that are controlled by the solvent dynamics.

Acknowledgment. We thank the Australian Research Council for support and for the award of a senior research fellowship to M.N.P.-R. We thank the Australian Partnership for Advanced Computing (APAC) and the Australian Centre for Advanced Computing and Communications (ac3) for allocation of computing time. D.H.W. acknowledges support from the U.S. National Science Foundation (CHE-0111435).

Supporting Information Available: Detailed synthetic procedures and the analogue of Figure 4 for compound **2**. This material is available free of charge via the Internet at http://pubs.acs.org.

JA049539D

(22) (a) Davidson, V. L. *Acc. Chem. Res.* **2000**, *33*, 87. (b) Davidson, V. L. *Biochemistry* **2000**, *39*, 4924. (c) Jeuken, L. J. C. *Biochim. Biophys. Acta−Bioenergetics* **2003**, *1604*, 67.